

See discussions, stats, and author profiles for this publication at: <https://www.researchgate.net/publication/268281033>

# Spectroscopic and thermodynamic properties of recombinant heat shock protein A6 from *Camelus dromedarius*

ARTICLE *in* EUROPEAN BIOPHYSICS JOURNAL · NOVEMBER 2014

Impact Factor: 2.22 · DOI: 10.1007/s00249-014-0997-2 · Source: PubMed

---

READS

60

8 AUTHORS, INCLUDING:



[Ajamaluddin Malik](#)

King Saud University

23 PUBLICATIONS 77 CITATIONS

SEE PROFILE



[Wajahatullah Khan](#)

King Saud bin Abdulaziz University for Heal...

57 PUBLICATIONS 932 CITATIONS

SEE PROFILE



[Mohammad Bazzi](#)

King Saud University

45 PUBLICATIONS 1,563 CITATIONS

SEE PROFILE

# Spectroscopic and thermodynamic properties of recombinant heat shock protein A6 from *Camelus dromedarius*

Ajamaluddin Malik · Abuzar Haroon · Haseeb Jagirdar ·  
Abdulrahman M. Alsenaidy · Mohamed Elrobh · Wajahatullah Khan ·  
Mohammed S. Alanazi · Mohammad D. Bazzi

Received: 11 June 2014 / Revised: 28 October 2014 / Accepted: 29 October 2014  
© European Biophysical Societies' Association 2014

**Abstract** Heat shock protein A6, also known as HSP70B', is a member of the Hsp70 family of molecular chaperones. Under stressed conditions, the level of HSPA6 increases substantially, and the protein has been targeted as a biomarker of cellular stress in several studies. We report the spectroscopic and thermodynamic properties of Arabian camel species cHSPA6, determined by measurement of intrinsic and extrinsic fluorescence emission, and use of far-UV circular dichroism and dynamic multimode spectroscopy. Our results showed that cHSPA6 has similar binding affinity for both ATP and ADP ( $K_D = \sim 50$  nM). Binding of ATP and ADP reduced the surface hydrophobicity of the protein, and slightly altered its secondary

structure, suggesting localized conformational rearrangement after ATP or ADP binding. Dynamic multimode spectroscopy revealed that cHSPA6 unfolds through three transitions with melting points ( $T_m$ ) of  $42.3 \pm 0.2$ ,  $61.3 \pm 0.1$ , and  $81.2 \pm 0.2$  °C. To the best of the author's knowledge, and literature search, this is the first report of the spectroscopic and thermodynamic properties of the Arabian camel heat shock protein.

**Keywords** Recombinant protein · Heat shock protein · Protein stability · Folding · Fluorescence quenching · Dynamic multimode spectroscopy

## Abbreviations

Amp	Ampicillin
DTT	Dithiothreitol
EDTA	Ethylenediaminetetraacetic acid
Em	Emission
Ex	Excitation
FPLC	Fast protein liquid chromatography
GdnHCl	Guanidinium hydrochloride
IPTG	Isopropyl $\beta$ -D-1-thiogalactopyranoside
$K_D$	Dissociation constant
LB	Luria–Bertani
2XLB	Double strength Luria–Bertani
NB	Nutrient broth
MWCO	Molecular weight cut off
Ni-NTA	Nickel-nitrilotriacetic acid
NBD	Nucleotide binding domain
OD <sub>600</sub>	Optical density at 600 nm
PMSF	Phenylmethylsulfonyl fluoride
rpm	Rotation per minute
SBD	Substrate binding domain
TB	Terrific broth
$T_m$	Melting temperature

A. Malik (✉) · H. Jagirdar · A. M. Alsenaidy · M. D. Bazzi  
Protein Research Chair, Department of Biochemistry, College  
of Science, King Saud University, PO Box 2455, Riyadh 11451,  
Saudi Arabia  
e-mail: amalik@ksu.edu.sa

A. Haroon  
Tabuk Pharmaceuticals Manufacturing Co., P.O. Box 4640,  
2nd Industrial City, Dammam 31421, Saudi Arabia

M. Elrobh · M. S. Alanazi · M. D. Bazzi  
Genome Research chair, Department of Biochemistry, College  
of Science, King Saud University, PO Box 2455, Riyadh 11451,  
Saudi Arabia

M. Elrobh  
Biochemistry Department, Faculty of Science, Ain-Shams  
University, Abbassia, 11381 Cairo, Egypt

W. Khan  
Department of Basic Sciences, College of Science and Health  
Professions, King Saud Bin Abdulaziz University for Health  
Sciences, PO Box 3660, Riyadh 11426, Saudi Arabia

## Introduction

The Arabian camel (*Camelus dromedaries*) is one of few mammals which can survive under conditions of intense heat and dryness. Surrounding temperatures have large effects on the biochemistry and physiology of all organisms at the molecular level. The native structure of proteins is stabilized by different types of relatively weak non-covalent interaction, for example hydrogen bonding, and hydrophobic, ionic, and dipole–dipole interactions (Dill 1990). At high temperatures, however, the vibration of atoms in proteins increases and breaks the weak non-covalent bonds (Vogt et al. 1997), resulting in denaturation and loss of protein function. Proteins are synthesized in a highly crowded cytosolic environment (>200 mg/ml proteins); at such a high level of molecular crowding, incorrect interactions may lead to misfolding and aggregation and/or proteolysis of newly synthesized proteins (Brown 1991; Tavaría et al. 1996).

Heat shock proteins are of crucial importance in the folding and stability of almost all proteins (Liu et al. 2010) and are usually expressed under extreme environmental conditions, for example biotic and abiotic stresses, including high temperatures (Santoro 2000). It is fair to assume that the Arabian camel that lives under extreme hot and dry climatic conditions must face extra challenges with regard to protein folding and functioning.

The key function of heat shock proteins in living cells and organisms is to provide stability to protein homeostasis. The Hsp70 class of chaperones enables an organism to adapt to a variety of environmental, developmental, and physiological stresses (Mayer and Bukau 2005). In *E. coli*, it has been observed that deletion of Hsp70 chaperone results in aggregation of more than 300 different proteins (Deuerling et al. 2003). In eukaryotes, the Hsp70 chaperones make up 1–2 % of total protein (Zylicz et al. 2001) and assist in the folding of thousands of cellular proteins (Mayer and Bukau 2005). Hsp70 chaperones actively participate in several other cellular processes, including transportation of proteins across membranes (Borges and Ramos 2005; Walter and Buchner 2002), cardiovascular diseases (Benjamin and McMillan 1998), immunity (Nishikawa et al. 2008), and apoptosis (Beere et al. 2000). Hsp70 chaperones are a fertile area for biomedical research and have been targeted for development of therapeutic proteins (Zylicz et al. 2001).

HSPA6, also known as HSP70B', is a member of Hsp70 family of molecular chaperones. Members of Hsp70 are crucially involved in maintaining cellular proteostasis (Heldens et al. 2010). Under unstressed conditions, expression of HSPA6 cannot be detected (Leung et al. 1990; Parsian et al. 2000). Under stressed conditions, however, its level increases substantially, and it has been used as

biomarker in several cellular stress studies (Wada et al. 2005; Wang et al. 2005). Structurally, Hsp70 chaperones are highly conserved, monomeric, two-domain proteins. The larger N-terminal domain (~45 kDa) is known as the nucleotide binding domain (NBD) whereas the smaller C-terminal domain (25 kDa) is the substrate-binding domain (SBD); the domains are connected by a short, flexible, hydrophobic linker (Flaherty et al. 1990). Chaperones of Hsp70 members have been studied extensively but their mechanism of action is not completely understood (Bukau and Horwich 1998; Morano 2007). It has been suggested that the Hsp70 chaperones temporarily bind to hydrophobic residues of the proteins under stress, prevent partially-denatured proteins from aggregation, and assist them in refolding. Results obtained so far indicate that NBD and SBD interact in an allosteric regulatory fashion. Crucial residues involved in the allosteric regulation have been identified (Rist et al. 2006; Vogel et al. 2006). Binding of ATP to the NBD can induce conformational change in the SBD which leads to release of the substrate. In contrast, binding of the substrate to the SBD enhances the ATPase activity of the NBD (Buchberger et al. 1995; Moro et al. 2003; Revington et al. 2005; Swain et al. 2007).

In this study we report overexpression of cHSPA6 in *E. coli*, and its subsequent purification. Studies of nucleotide-binding by use of fluorescence-quenching methods revealed high affinity ( $K_D \sim 50$  nM). Far-UV CD measurements in the nucleotide-bound state revealed small changes of secondary structure. Structural and thermodynamic properties were characterized by use of dynamic multi-mode spectroscopy. Similar to DnaK of *E. coli* (EcDnaK) and human Hsc70, cHSPA6 also unfolds via three thermal transitions. Interestingly, in the nucleotide-bound state, the conformational state of cHSPA6 is more similar to that of human Hsc70 than to that of EcDnaK.

## Materials and methods

### Materials

The vector pET15-cHSPA6 encoding Arabian camel HSPA6, characterization of which has been reported elsewhere (Elrobh et al. 2011), was kindly provided by Dr Elrobh (Department of Biochemistry, King Saud University, KSA). *E. coli* BL21 (DE3) pLysS was obtained from Life Technologies. Benzonase was purchased from Sigma and chicken egg lysozyme was purchased from USB Corporation. IPTG and ampicillin were obtained from Biobasic. Ni-NTA resin, Superdex 75 prepacked columns, and low molecular weight markers were purchased from Amersham Biosciences. Other chemicals were reagent grade.

## cHSPA6 expression and purification

cHSPA6 fused with a hexa-histidine tag at the N-terminus was cloned on pET15 under strong T7 promoter. For protein expression, pET15-cHSPA6 plasmid was transformed into *E. coli* BL21 (DE3) pLysS. To prepare biomass, 1 % overnight culture was transferred to 1 l LB<sub>amp</sub> (200 µg/ml) in 6-l conical flasks. cHSPA6 expression was induced by adding 25 µM IPTG when growth reached the mid-exponential phase ( $OD_{600} = 0.6$ ). After post-induction incubation for 5 h, cells were harvested at 5,000 rpm for 15 min. The biomass (2.5 g) was resuspended in 15 ml lysis buffer (50 mM Tris, 200 µM PMSF, 3 mM DTT, 2 mM MgCl<sub>2</sub>, and 300 µg/ml lysozyme, pH 7.5). The biomass was homogenized in a mechanical homogenizer to a uniform slurry then 1 µl benzonase (250 U/µl) was added to the slurry and the mixture was incubated at room temperature for 1 h. The slurry was then subjected to mild sonication (Soniprep 150; MSE UK), twice, each time for 10 s, at 5 µm amplitude and 4 °C. Next, the slurry was centrifuged for 30 min at 13,000 rpm at 4 °C. Supernatant was collected and filtered through a 0.45 µm filter. Sodium chloride was added to the filtrate to achieve a final concentration of 500 mM. Further imidazole was added to the solution to bring the final concentration to 10 mM. The supernatant was passed through a 1-ml HisTrap column which had previously been equilibrated with 20 ml equilibration buffer (50 mM Tris, 10 mM imidazole, and 500 mM NaCl, pH 7.5). The column was connected to a fast protein liquid chromatography (FPLC) system. After washing with equilibration buffer until the absorbance at 280 nm reached baseline level, the His-tagged cHSPA6 was eluted with a gradient of 0–50 % with elution buffer (50 mM Tris, 500 mM, imidazole, and 500 mM NaCl, pH 7.5) at 0.5 ml/min. The purity of cHSPA6 in different fractions was checked on 12 % SDS gel. The fractions containing cHSPA6 were combined and loaded on to a Superdex 75 26/60 column pre-equilibrated with 25 mM Tris and 250 mM NaCl, pH 7.5. The purity of the fractions was analyzed on 12 % SDS gel. The buffer of the purified cHSPA6 was exchanged in 4 cycles with 20 mM sodium phosphate buffer containing 50 mM NaCl at pH 7.4, by use of Centricon (MWCO 10,000 Da). The permeate from the fourth cycle was used as reference control in spectroscopic studies.

## Sequence alignment and prediction of the 3D structure of cHSPA6

cHSPA6 (accession number HQ214118.1), human HSP70B' (BAD97082.1), and bovine HSPA6 (XP\_589747.1) were used for multiple sequence alignment by ClustalW on MAFFT multiple sequence alignment program. Output is reported in accordance with the conserved sequence. The amino acid

sequence of cHSPA6 (accession number HQ214118.1) was used to predict 3D structure by use of the ITASSER server based on multiple-threading alignments by LOMETS and iterative TASSER assembly simulations (Roy et al. 2010).

## UV–visible spectroscopy

UV–visible spectra of cHSPA6 were recorded from 250 to 700 nm at 20 °C, by use of an Ultrospec 2,100 Pro UV–visible spectrophotometer (Amersham Pharmacia Biotech). A quartz cell with 10-mm path length was used. Protein concentration was calculated by use of a cHSPA6 molar extinction coefficient of 34,840.

## Fluorescence spectroscopy

Fluorescence of 2 µM cHSPA6, at 20 °C, was recorded by use of a Jasco FP-750 spectrofluorimeter with a 10-mm path length quartz cell; the excitation and emission slit widths were 5 nm. The emission spectra of native and 6 M GdnHCl-denatured cHSPA6 were measured by excitation at 280 nm and recording emission between 300 and 400 nm. Conformational transitions of cHSPA6 induced by different concentrations of ATP and ADP were recorded by excitation at 280 nm and recording emission between 295 and 400 nm. The fluorescence signal at 335 nm was used to calculate percentage quenching by use of the equation:

$$\% \text{ quenching} = (F_0 - F) \times 100/F_0$$

where  $F_0$  and  $F$  represent fluorescence intensity in the absence and presence of quencher, respectively.

ANS (8-anilino-1-naphthalenesulfonic acid) binding was measured, at 20 °C, by use of a Jasco FP-750 spectrofluorimeter with a 10-mm path length cuvette; the excitation and emission slit widths were 5 nm. Samples were excited at 375 nm and emission was recorded between 450 and 510 nm. The cuvette containing 100 µM ANS was pre-equilibrated with 2 µM cHSPA6 before nucleotide binding was started. Twofold serially diluted ATP or ADP solutions (2 µl) were inoculated and equilibrated before each measurement. Final dilution was less than 3 %. Changes in cHSPA6 hydrophobic surfaces as a result of the conformational change induced by nucleotide binding were estimated by ANS binding.

## Circular dichroism

Circular dichroism measurements were performed, at 20 °C, with a Chirascan-Plus CD spectrophotometer (Applied Photophysics, Leatherhead, UK) coupled with Peltier temperature controller. The CD instrument was calibrated with (1S)-(+)-10-camphorsulfonic acid. To measure far-UV spectra, the monochromator was set at 260 nm with 1 nm bandwidth and

data were collected at 0.5 s per point. Five scans of the CD spectra of 3  $\mu$ M cHSPA6 in 10 mM sodium phosphate buffer, pH 7.5, containing 50 mM NaCl were performed between 200 and 260 nm in the presence and absence of 0.66 mM nucleotides (ATP and ADP). Air baseline and buffer background were subtracted. The data were analyzed by use of Chirascan's Pro-data viewer. The path length was 1 mm and CD results were expressed in millidegrees (mdeg). Far-UV CD spectra were deconvoluted by use of the CDNN software package (version 2.1) provided by Applied Photophysics.

Dynamic multi-mode spectroscopy was performed with a Chirascan-Plus spectrophotometer, in accordance with the manufacturer's instructions. Briefly, temperature-dependent conformational changes were measured for 3  $\mu$ M cHSPA6 in 10 mM sodium phosphate buffer, pH 7.5, containing 50 mM NaCl. The CD spectra were recorded between 200 and 250 nm. The temperature was increased gradually from 20 to 94  $^{\circ}$ C, at a precise rate of 1  $^{\circ}$ /min. Thermal transition data were analyzed by use of Chirascan's Global 3 software.

## Results and discussion

### cHSPA6 structure

The (His)<sub>6</sub>-tag was fused at the N-terminus of cHSPA6 and a highly specific protease cleavage site (TEV protease) was placed between the (His)<sub>6</sub>-tag and cHSPA6 to enable

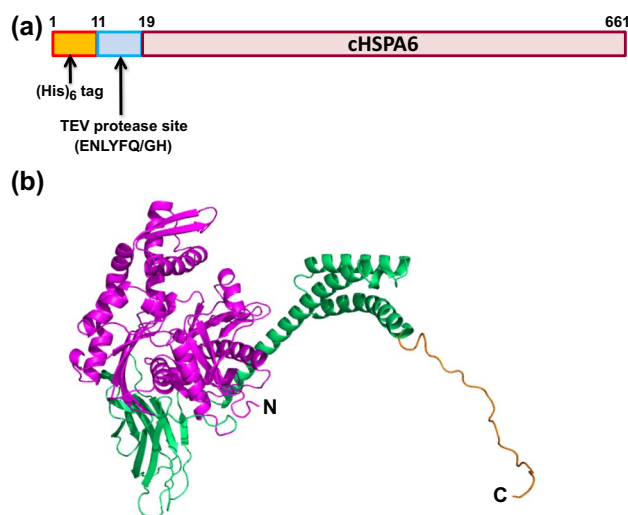


**Fig. 1** Design of the cHSPA6 fusion protein. **a** Schematic diagram of the His-tagged cHSPA6 fusion protein. Amino acid numbering starts with the N-terminus of the His-tag (1–10), followed by the highly specific TEV protease cleavage site (11–18) and cHSPA6 (19–661). **b** 3D structure of cHSPA6 modeled by use of multiple-threading alignments by LOMETS. N-terminal NBD is shown in magenta and the C-terminal SBD is shown in green. The last 24 residues of SBD have a highly flexible, structureless conformation, shown in orange

removal of the (His)<sub>6</sub>-tag after purification (Fig. 1a). The recombinant cHSPA6 fusion structure was 1983 nucleotides in length, corresponding to 661 amino acids or 72.7 kDa. The modeled 3D structure of cHSPA6 contained two domains (Fig. 1b). The N-terminal domain containing NBD has an  $\alpha$ -helix and  $\beta$ -sheet structure whereas the C-terminal domain containing SBD has an  $\alpha$ -helix-rich structure with a 24 amino acid-long stretch of an unstructured flexible C-terminus. The amino acid sequence of cHSPA6, when aligned with human HSP70B' (BAD97082.1) or bovine HSPA6 (XP\_589747.1) had 93 and 94 % sequence homology, respectively. The proteins had two conserved tryptophans and 14 conserved tyrosines (Tyr547 was an exception). One tryptophan residue is located in each domain whereas tyrosine residues were well distributed across the sequence.

### Expression and purification recombinant cHSPA6

The cHSPA6 was expressed by *E. coli* BL21(DE3) pLysS and subsequently purified, as described in the “Materials and methods” section. *E. coli* BL21(DE3) pLysS strain is lysogenic for the  $\lambda$ -DE3 cassette which expresses T7 RNA polymerase under the control of the IPTG-inducible lac-UV5 promoter. It also contains the pLysS plasmid to suppress the leakiness of cHSPA6 (Moffatt and Studier 1987). To obtain monomeric cHSPA6 species from higher-order structures and aggregated forms, the Ni-NTA elute was subjected to size-exclusion chromatography. Because it is well known that the HSP70 family of proteins have a tendency to dimerize and oligomerize, especially upon storage at low ionic strength (Borges and Ramos 2006; Schonfeld and Behlke 1998), a fresh preparation of cHSPA6 was made for spectroscopic studies. Highly pure cHSPA6 was obtained after size-exclusion chromatography (Fig. 2). After further purification, 9 mg highly purified cHSPA6 was obtained, corresponding to 3.6 mg per gram wet biomass.

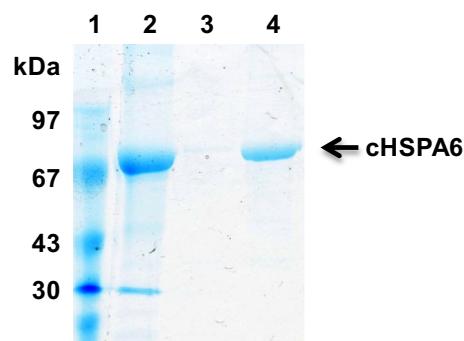


**Fig. 2** Purification of cHSPA6. Ni-NTA eluate was purified by size exclusion chromatography to obtain the monomeric form of cHSPA6. The purity of the Superdex 75 eluate was analyzed by Coomassie Blue staining. Lane 1, low molecular weight marker; lane 2, Ni-NTA eluate; lane 3, blank; lane 4, gel filtration eluate



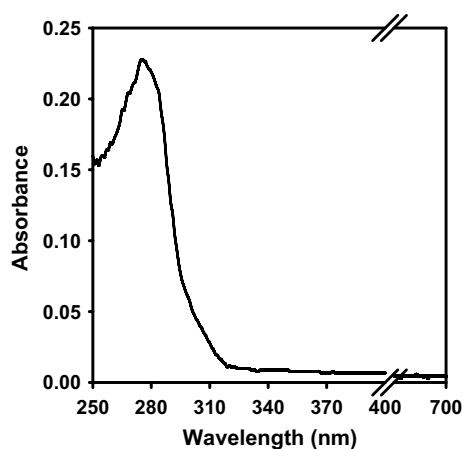


**Fig. 3** The UV–visible spectrum of purified cHSPA6 contained a single peak indicative of the ligand-free form of the protein

UV–visible spectroscopy confirmed production of pure protein

Recombinant cHSPA6 contains two tryptophan residues (W92 and W582) which are located in NBD and SBD, respectively. The cHSPA6 also contains 16 tyrosines and 25 phenylalanine residues which are distributed throughout

the primary structure. The UV–visible spectrum in the range 250–700 nm contained a single peak at 275 nm because of the dominance of tyrosine absorption (Fig. 3). The UV–visible spectrum is characteristic of soluble protein with no additional bound chromophores.

#### Fluorescence spectroscopy-indicated nucleotide binding

Recombinant cHSPA6 is a tyrosine-rich protein (Fig. 4). The fluorescence spectrum (excitation at 280 nm) was indicative of complex emission, with distinct peaks at 310 and 334 nm. This is probably because of the presence of 16 tyrosines and two tryptophans. The emission spectra of proteins containing both tryptophan and tyrosine residues are usually dominated by tryptophan fluorescence, even for proteins with a high tyrosine content, for example human serum albumin (one Trp and seventeen Tyr residues) (Teale 1960). Occasionally, however, for example the 33-kDa protein from spinach photosystem II (contains one Trp and eight Tyr residues), wheat alpha-purothionin (zero Trp and five Tyr), and crambin (zero Trp and two Tyr residues), the tyrosine emission spectrum has been observed (Prendergast et al. 1984; Ruan et al. 2002). Therefore, native cHSPA6 may belong to latter group of proteins, because its emission spectrum contained peaks corresponding to tyrosine

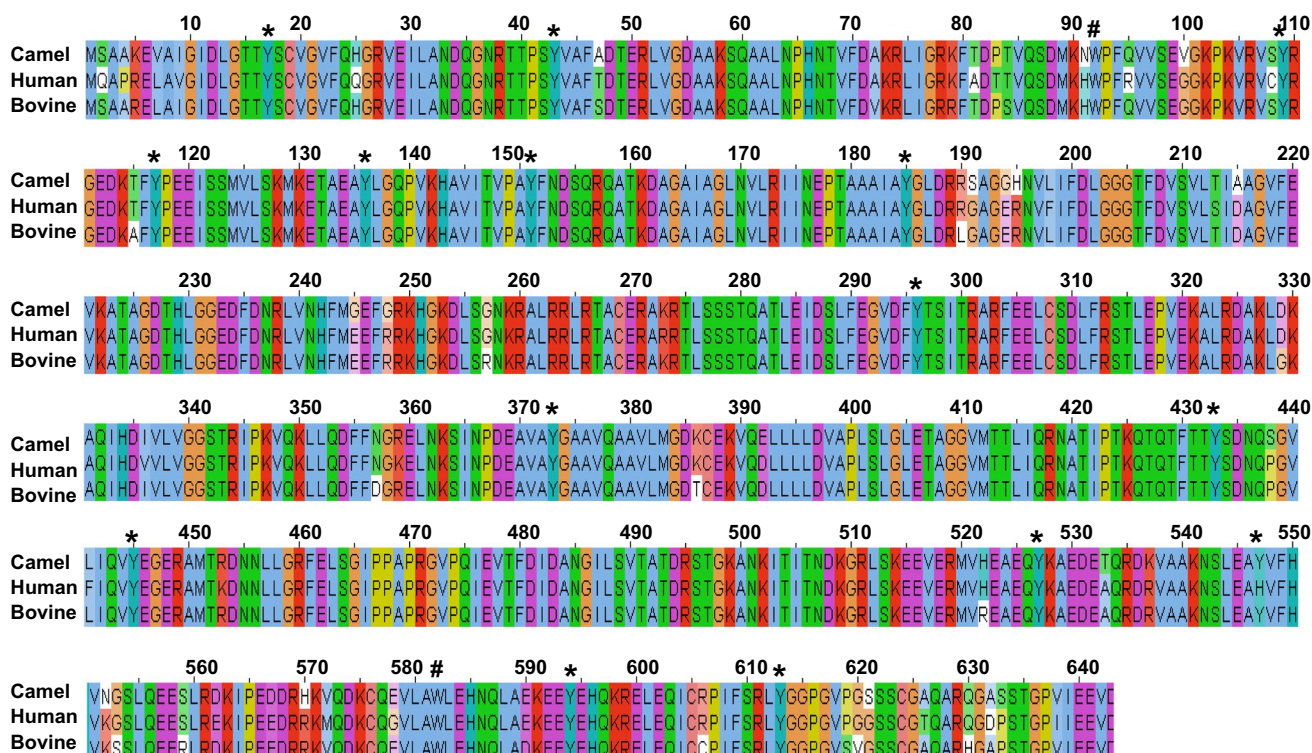


**Fig. 4** Amino acid sequence alignment. Camel HSPA6 (accession number HQ214118.1), human HSP70B (BAD97082.1), and bovine HSPA6 (XP\_589747.1) were aligned by use of MAFFT multiple

sequence alignment software. Conserved tryptophans are indicated with hash symbols and all the tyrosines were conserved, indicated with asterisk symbols, except Tyr 547

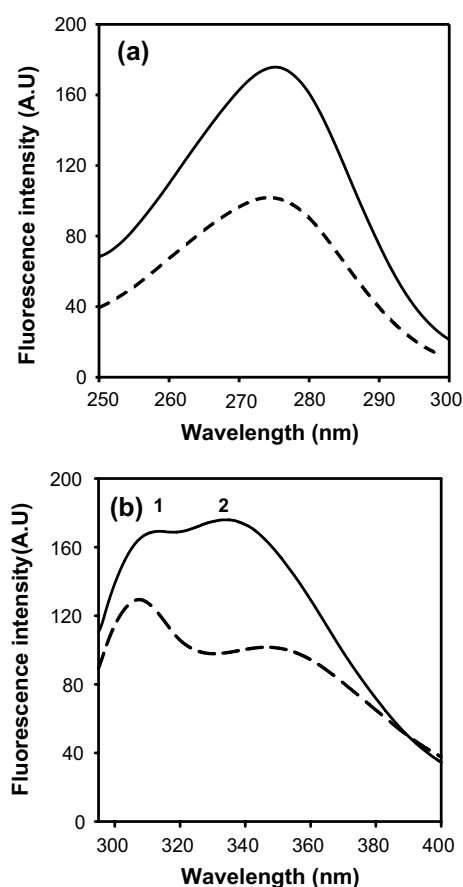


**Fig. 5** Intrinsic fluorescence spectra of native and denatured cHSPA6. **a** Excitation spectra of cHSPA6 in the native (*solid line*) and denatured (*broken line*) states recorded between 250 and 300 nm, Em 340 nm. Ex maximum was at 275 nm, because of the high tyrosine content. **b** Emission spectra measured at 280 nm, which excites both tryptophan and tyrosine residues. Two peaks are present: *peak 1* is tyrosine emission spectra and *peak 2* is tryptophan emission. The *solid line* is the emission spectrum of cHSPA6 in the native state and the *broken line* is that of the denatured state. When cHSPA6 was denatured,  $\lambda_{\text{max}}$  of the second peak was red-shifted 14 nm because of the polarity-sensitive nature of tryptophan emission

and tryptophan emission (Fig. 5). When cHSPA6 was denatured, the 334 nm peak was red shifted to 346 nm, because of the environment-sensitive nature of tryptophan. (Edelhoch 1967; Rao et al. 1981). Moreover, when cHSPA6 was excited at 295 nm, the amplitude of the peak at 310 nm was substantially reduced (data not shown), further supporting the conclusion that the 310 nm peak corresponded to tyrosine emission whereas the 334 nm peak corresponded to tryptophan emission.

The results in Fig. 6a indicate that ATP and ADP quenched cHSPA6 total fluorescence. The tryptophan (Trp92) of cHSPA6 located in the NBD must be sensitive to the conformational changes induced by ATP or ADP binding. In previous studies, ATP binding to HSP70 member proteins resulted in fluorescence quenching

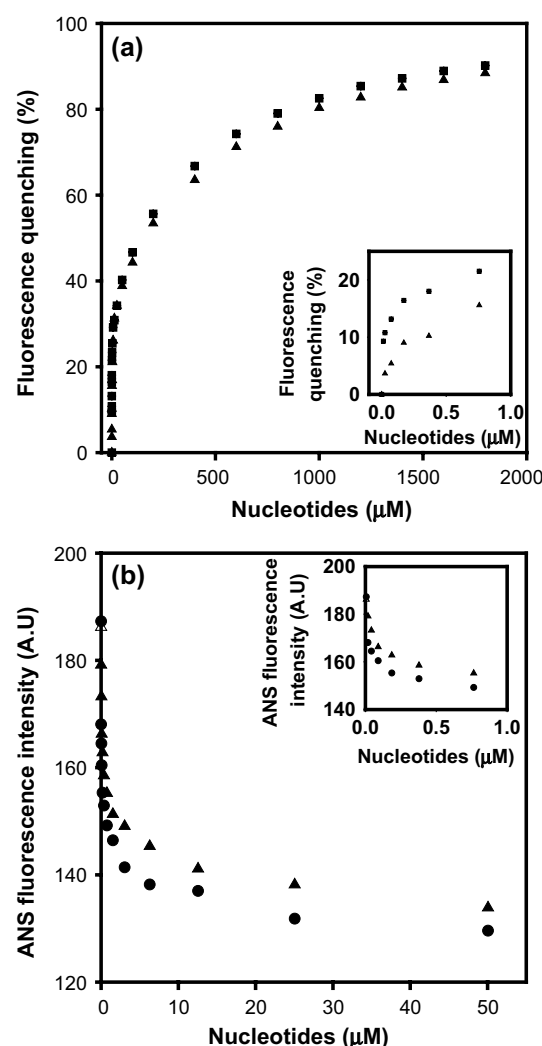


**Fig. 6** Nucleotide-induced change in the conformation of cHSPA6. **a** Intrinsic fluorescence quenching of 2  $\mu\text{M}$  cHSPA6 in response to increasing concentration of ATP (*closed triangles*) and ADP (*closed squares*). Emission spectra were obtained by exciting at 280 nm, and emission at  $\lambda_{\text{max}}$  334 nm was used for calculating fluorescence quenching. **b** ANS fluorescence measurement in the presence of increasing concentrations of ATP (*closed triangles*) and ADP (*closed squares*). 2  $\mu\text{M}$  cHSPA6 was mixed with 100  $\mu\text{M}$  final ANS concentration. Changes in surface hydrophobicity as a result of increasing nucleotide concentrations were monitored by exciting at 375 nm. The *insets* in both figures show the fluorescence quenching and ANS fluorescence in response to nM concentrations of nucleotides

(Banecki et al. 1992; Theyssen et al. 1996). Reported  $K_D$  of mammalian Hsc70 ranges from 12 nM to 9.5  $\mu\text{M}$  for ATP and from 18 nM to 1.6  $\mu\text{M}$  for ADP. The dissociation constant of prokaryotic (*E. coli*, *T. thermophilus*) DnaK ranges from 1 to 47 nM for ATP and from 47 to 130 nM for ADP (Borges et al. 2005; Gao et al. 1994; Ha and McKay 1994; Huang et al. 1993; Klostermeier et al. 1998; Palleros et al. 1991; Russell et al. 1998; Theyssen et al. 1996). The precise affinity of Hsp70 for nucleotides

varies, because of large differences among ATP release rate for members of the Hsp70 family (Mayer et al. 2001; Wegele et al. 2004). Our results show cHSPA6 has similar affinity for ADP and ATP, in agreement with those of Gao et al. (1994). Higher affinity for ATP (Ha and McKay 1994; Theyssen et al. 1996) or for ADP (Palleros et al. 1991) have also been reported. This different affinity is probably because of the different functional diversity of Hsp70 members and the different techniques used for investigation.

Variations in surface hydrophobicity of cHSPA6 as a result of binding of ATP or ADP to the NBD were determined by use of an extrinsic fluorescent probe. The fluorescent dye 8-anilino-1-naphthalenesulfonic acid (ANS) is widely used to measure exposure of surface hydrophobicity during the course of conformational change (Walmsley et al. 1994). As shown in Fig. 6b, ATP and ADP binding both lead to changes in conformation, as is apparent from the loss of the ANS signal because of the decrease in surface hydrophobicity. Thus fluorescence spectroscopy reveals that ATP and ADP binding in the nanomolar range lead to conformational changes in cHSPA6.

#### Circular dichroism-characterized nucleotide-induced changes in the conformation of cHSPA6

cHSPA6 is an  $\alpha$ -helix-rich structural protein, as demonstrated by its far-UV CD spectra (Figs. 1b, 7). Our results showed that ATP binding led to an increase in  $\alpha$ -helix structure whereas in the ADP-bound state the  $\alpha$ -helix structure was less than in the unbound state. One possibility is that the conformation of Hsp70 switches between

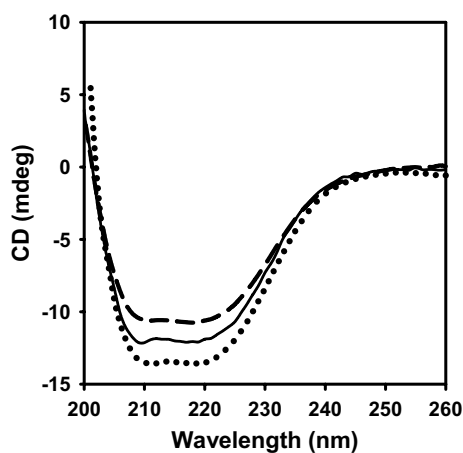


**Fig. 7** Far-UV CD spectra of cHSPA6 in the presence of the nucleotides. Changes in the secondary structure induced by nucleotide binding were monitored by far-UV CD. The *solid line* is the spectrum of 3  $\mu$ M cHSPA6 in the absence of nucleotide; the *dotted line* is the spectrum in the presence of 0.66 mM ATP; the *dashed line* is the spectrum in the presence of 0.66 mM ADP

**Table 1** Alpha-helix content of cHSPA6 in the presence and absence of nucleotides, calculated from 200 to 260 nm CD spectra by use of CDNN

Protein	$\alpha$ -Helix content (%)
cHSPA6	22.90
cHSPA6 + ATP	24.40
cHSPA6 + ADP	20.40

the ATP-bound open conformation and the ADP-bound closed state. When ATP binds, Hsp70 assumes a substrate-binding-site-open conformation. After hydrolysis of ATP to ADP, Hsp70 undergoes structural changes in which the substrate-binding site is in the closed state and the substrates are trapped (Freeman et al. 1995; Wu et al. 2001). In-vitro experiments have shown that Hsp70 proteins have affinity for misfolded proteins and small peptides. They also have weak ATPase activity. Binding of ATP induces conformational changes and results in release of the peptides (Flynn et al. 1989; Gragerov et al. 1994; Mayer et al. 2001; Palleros et al. 1993).

The  $\alpha$ -helix content of the secondary structure in cHSPA6 in the presence or absence of nucleotides was estimated from far-UV CD spectra by use of CDNN CD software (Table 1) (Bohm et al. 1992). Binding of ATP resulted in an increase in  $\alpha$ -helix content (Table 1, Fig. 7). Similar conformational changes in the presence of ATP have also been observed for EcDnaK by use of infrared spectroscopy and time-resolved infrared difference spectroscopy (Banecki et al. 1992; Moro et al. 2006). Interestingly, ATP binding with EcDnaK leads to quenching and conformational changes but ADP binding neither quenches EcDnaK fluorescence nor induces conformational change. However, human Hsc70 undergoes conformational changes when bound to ADP (Wu et al. 1985). ATP induces conformational changes in both human Hsc70 and EcDnaK. However, ADP binding leads to conformational change of human Hsc70 but not of EcDnaK. Such changes might lead to functional diversity in the chaperoning system (Borges et al. 2005; Cheetham and Caplan 1998; Fan et al. 2004).

#### Dynamic multimode spectroscopy

Dynamic multimode spectroscopy is a newly developed, information-rich experimental technique which furnishes structural and thermodynamic data. To calculate the thermodynamics of unfolding and the mid-points of unfolding transitions, CD spectra between 200 and 250 nm of cHSPA6 in the nucleotide-free state were recorded as a function of temperature. Figure 8a shows the protein underwent three well-defined thermal transitions as a function of temperature, suggesting four folding states. The CD spectra

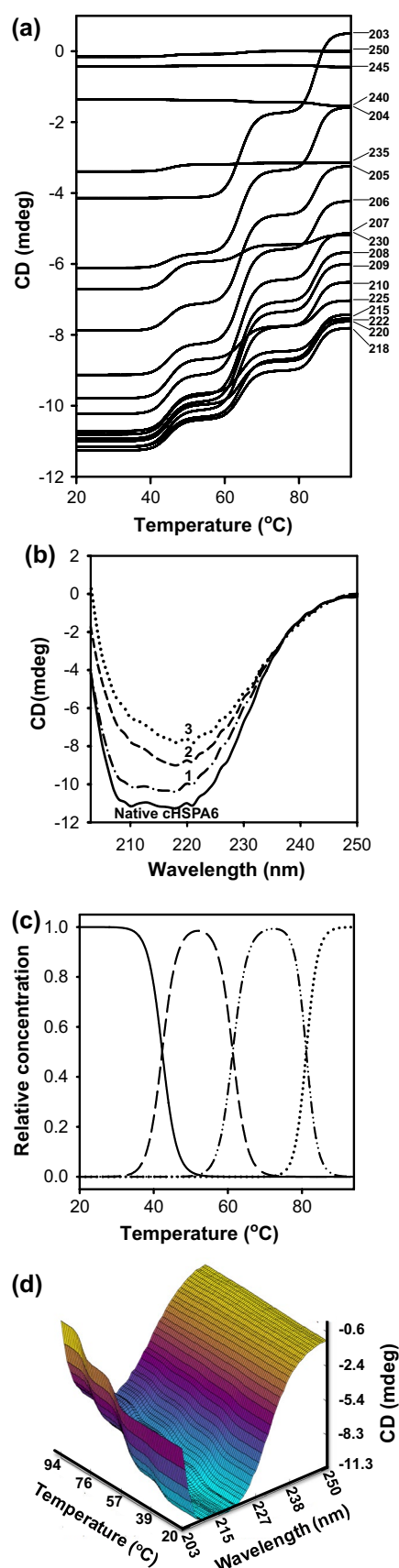


**Fig. 8** Far-UV CD as a function of temperature and wavelength. **a** ▶ Temperature-dependent conformation changes at different wavelengths. CD values in mdeg units at different wavelengths in the far-UV region were plotted as a function of temperature. Global 3 analysis software, especially developed by Applied Photophysics for dynamic multimode spectroscopy, was used for determination of the thermal transitions. The wavelengths are indicated on the *right Y axis*. Three thermal transitions are clearly seen at wavelengths between 204 and 225 nm. **b** Calculated far-UV CD spectra of the contributing species. At low temperature cHSPA6 adopts an  $\alpha$ -helix conformation. The *plots* show the CD spectra of the species if they were the sole contributors on completion of a thermal transition. With increasing temperature, cHSPA6 loses the  $\alpha$ -helix conformation, and unfolding species 2 and 3 are the more beta-strand-rich structures. **c** Calculated concentration profiles of the folding species. The *graph* shows the temperature-dependent disappearance and appearance of the species and their relative concentrations. **d** Calculated temperature–wavelength and CD surface. The 3D model was calculated by use of Global 3 software by using CD values obtained at increasing temperatures in the far-UV region

indicated gradual conversion of the alpha-helix rich structure into a  $\beta$ -sheet dominant structure as the temperature was increased (Fig. 8b). The relative concentrations of the different folding states as a function of temperature are shown in Fig. 8c. The melting points calculated by use of Global 3 analysis software were  $42.3 \pm 0.2$ ,  $61.3 \pm 0.1$ , and  $81.2 \pm 0.2$  °C. DSC study of DnaK revealed three unfolding transitions in the nucleotide-free state, with  $T_m$  values close to 45.2, 58, and 73.3 °C (Montgomery et al. 1999). Thermally induced unfolding of human Hsc70 also occurred via three transitions, with  $T_m$  of 46, 68, and 82 °C (Palleros et al. 1991); as a result of unfolding of the NBD and SBD and collapse of the remaining structures in the N and C-terminal domains (Montgomery et al. 1999). The NBD domain of cHSPA6 is slightly less stable than those of the bacterial DnaK and human Hsc70 counterparts, whereas the stability of cHSPA6 SBD is between those of DnaK and Hsc70. A 3D model of the thermal transitions in cHSPA6 was generated by use of Global 3 analysis software (Fig. 8d). Three transitions as a function of temperature are clearly apparent at low wavelengths.

## Conclusion

We have produced cHSPA6 by recombinant techniques and purified it to homogeneity in quantities sufficient to perform structural and thermodynamic studies. We observed via intrinsic fluorescence quenching that cHSPA6 had similar affinity for ATP or ADP. In ATP or ADP-bound cHSPA6 the hydrophobic surface was reduced. Far-UV CD measurements showed that cHSPA6 gains  $\alpha$ -helix structure in the ATP-bound state but loses  $\alpha$ -helix structure in the ADP-bound state. A similar conformational change in the



nucleotide bound state has also been observed for mammalian Hsp70. The cHSPA6 unfolds via three thermal transitions in a manner similar to that observed for *E. coli* and for humans.

**Acknowledgments** The authors extend their appreciation to King Abdulaziz City for Science and Technology (KACST), Riyadh, Saudi Arabia, for funding this work through project # A-C-11-0606.

## References

- Banecki B, Zyllicz M, Bertoli E, Tanfani F (1992) Structural and functional relationships in DnaK and DnaK756 heat-shock proteins from *Escherichia coli*. *J Biol Chem* 267:25051–25058
- Beere HM, Wolf BB, Cain K, Mosser DD, Mahboubi A, Kuwana T, Taylor P, Morimoto RI, Cohen GM, Green DR (2000) Heat-shock protein 70 inhibits apoptosis by preventing recruitment of procaspase-9 to the Apaf-1 apoptosome. *Nat Cell Biol* 2:469–475
- Benjamin IJ, McMillan DR (1998) Stress (heat shock) proteins: molecular chaperones in cardiovascular biology and disease. *Circ Res* 83:117–132
- Bohm G, Muhr R, Jaenicke R (1992) Quantitative analysis of protein far UV circular dichroism spectra by neural networks. *Protein Eng* 5:191–195
- Borges JC, Ramos CH (2005) Protein folding assisted by chaperones. *Protein Pept Lett* 12:257–261
- Borges JC, Ramos CH (2006) Spectroscopic and thermodynamic measurements of nucleotide-induced changes in the human 70-kDa heat shock cognate protein. *Arch Biochem Biophys* 452:46–54
- Borges JC, Fischer H, Craievich AF, Ramos CH (2005) Low resolution structural study of two human HSP40 chaperones in solution. DJA1 from subfamily A and DJB4 from subfamily B have different quaternary structures. *J Biol Chem* 280:13671–13681
- Brown GC (1991) Total cell protein concentration as an evolutionary constraint on the metabolic control distribution in cells. *J Theor Biol* 153:195–203
- Buchberger A, Theyssen H, Schroder H, McCarty JS, Virgallita G, Milkereit P, Reinstein J, Bukau B (1995) Nucleotide-induced conformational changes in the ATPase and substrate binding domains of the DnaK chaperone provide evidence for interdomain communication. *J Biol Chem* 270:16903–16910
- Bukau B, Horwich AL (1998) The Hsp70 and Hsp60 chaperone machines. *Cell* 92:351–366
- Cheetham ME, Caplan AJ (1998) Structure, function and evolution of DnaJ: conservation and adaptation of chaperone function. *Cell Stress Chaperones* 3:28–36
- Deuerling E, Patzelt H, Vorderwulbecke S, Rauch T, Kramer G, Schaffitzel E, Mogk A, Schulze-Specking A, Langen H, Bukau B (2003) Trigger Factor and DnaK possess overlapping substrate pools and binding specificities. *Mol Microbiol* 47:1317–1328
- Dill KA (1990) Dominant forces in protein folding. *Biochemistry* 29:7133–7155
- Edelhoch H (1967) Spectroscopic determination of tryptophan and tyrosine in proteins. *Biochemistry* 6:1948–1954
- Elrobb MS, Alanazi MS, Khan W, Abduljaleel Z, Al-Amri A, Bazzi MD (2011) Molecular cloning and characterization of cDNA encoding a putative stress-induced heat-shock protein from *Camelus dromedarius*. *Int J Mol Sci* 12:4214–4236
- Fan CY, Lee S, Ren HY, Cyr DM (2004) Exchangeable chaperone modules contribute to specification of type I and type II Hsp40 cellular function. *Mol Biol Cell* 15:761–773
- Flaherty KM, DeLuca-Flaherty C, McKay DB (1990) Three-dimensional structure of the ATPase fragment of a 70 K heat-shock cognate protein. *Nature* 346:623–628
- Flynn GC, Chappell TG, Rothman JE (1989) Peptide binding and release by proteins implicated as catalysts of protein assembly. *Science* 245:385–390
- Freeman BC, Myers MP, Schumacher R, Morimoto RI (1995) Identification of a regulatory motif in Hsp70 that affects ATPase activity, substrate binding and interaction with HDJ-1. *EMBO J* 14:2281–2292
- Gao B, Greene L, Eisenberg E (1994) Characterization of nucleotide-free uncoating ATPase and its binding to ATP, ADP, and ATP analogues. *Biochemistry* 33:2048–2054
- Gragerov A, Zeng L, Zhao X, Burkholder W, Gottesman ME (1994) Specificity of DnaK-peptide binding. *J Mol Biol* 235:848–854
- Ha JH, McKay DB (1994) ATPase kinetics of recombinant bovine 70 kDa heat shock cognate protein and its amino-terminal ATPase domain. *Biochemistry* 33:14625–14635
- Heldens L, Dirks RP, Hensen SM, Onnekink C, van Genesen ST, Rustenburg F, Lubsen NH (2010) Co-chaperones are limiting in a depleted chaperone network. *Cell Mol Life Sci* 67:4035–4048
- Huang SP, Tsai MY, Tzou YM, Wu WG, Wang C (1993) Aspartyl residue 10 is essential for ATPase activity of rat hsc70. *J Biol Chem* 268:2063–2068
- Klostermeier D, Seidel R, Reinstein J (1998) Functional properties of the molecular chaperone DnaK from *Thermus thermophilus*. *J Mol Biol* 279:841–853
- Leung TK, Rajendran MY, Monfries C, Hall C, Lim L (1990) The human heat-shock protein family. Expression of a novel heat-inducible HSP70 (HSP70B') and isolation of its cDNA and genomic DNA. *Biochem J* 267:125–132
- Liu C, Young AL, Starling-Windhof A, Bracher A, Saschenbrecker S, Rao BV, Rao KV, Bermingham O, Mielke T, Hartl FU, Beckmann R, Hayer-Hartl M (2010) Coupled chaperone action in folding and assembly of hexadecameric Rubisco. *Nature* 463:197–202
- Mayer MP, Bukau B (2005) Hsp70 chaperones: cellular functions and molecular mechanism. *Cell Mol Life Sci* 62:670–684
- Mayer MP, Brehmer D, Gassler CS, Bukau B (2001) Hsp70 chaperone machines. *Adv Protein Chem* 59:1–44
- Moffatt BA, Studier FW (1987) T7 lysozyme inhibits transcription by T7 RNA polymerase. *Cell* 49:221–227
- Montgomery DL, Morimoto RI, Gierasch LM (1999) Mutations in the substrate binding domain of the *Escherichia coli* 70 kDa molecular chaperone, DnaK, which alter substrate affinity or interdomain coupling. *J Mol Biol* 286:915–932
- Morano KA (2007) New tricks for an old dog: the evolving world of Hsp70. *Ann N Y Acad Sci* 1113:1–14
- Moro F, Fernandez V, Muga A (2003) Interdomain interaction through helices A and B of DnaK peptide binding domain. *FEBS Lett* 533:119–123
- Moro F, Fernandez-Saiz V, Muga A (2006) The allosteric transition in DnaK probed by infrared difference spectroscopy. Concerted ATP-induced rearrangement of the substrate binding domain. *Protein Sci* 15:223–233
- Nishikawa M, Takemoto S, Takakura Y (2008) Heat shock protein derivatives for delivery of antigens to antigen presenting cells. *Int J Pharm* 354:23–27
- Palleros DR, Welch WJ, Fink AL (1991) Interaction of hsp70 with unfolded proteins: effects of temperature and nucleotides on the kinetics of binding. *Proc Natl Acad Sci USA* 88:5719–5723
- Palleros DR, Reid KL, Shi L, Welch WJ, Fink AL (1993) ATP-induced protein-Hsp70 complex dissociation requires K<sup>+</sup> but not ATP hydrolysis. *Nature* 365:664–666
- Parsian AJ, Sheren JE, Tao TY, Goswami PC, Malyapa R, Van Rheeden R, Watson MS, Hunt CR (2000) The human Hsp70B

- gene at the HSPA7 locus of chromosome 1 is transcribed but non-functional. *Biochim Biophys Acta* 1494:201–205
- Prendergast FG, Hampton PD, Jones B (1984) Characteristics of tyrosinate fluorescence emission in alpha- and beta-purothionins. *Biochemistry* 23:6690–6697
- Rao MV, Atreyi M, Rajeswari MR (1981) Fluorescence spectra of lysozyme excited at 305 NM in presence of urea. *Int J Pept Protein Res* 17:205–210
- Revington M, Zhang Y, Yip GN, Kurochkin AV, Zuiderweg ER (2005) NMR investigations of allosteric processes in a two-domain *Thermus thermophilus* Hsp70 molecular chaperone. *J Mol Biol* 349:163–183
- Rist W, Graf C, Bukau B, Mayer MP (2006) Amide hydrogen exchange reveals conformational changes in hsp70 chaperones important for allosteric regulation. *J Biol Chem* 281:16493–16501
- Roy A, Kucukural A, Zhang Y (2010) I-TASSER: a unified platform for automated protein structure and function prediction. *Nat Protoc* 5:725–738
- Ruan K, Li J, Liang R, Xu C, Yu Y, Lange R, Balny C (2002) A rare protein fluorescence behavior where the emission is dominated by tyrosine: case of the 33-kDa protein from spinach photosystem II. *Biochem Biophys Res Commun* 293:593–597
- Russell R, Jordan R, McMacken R (1998) Kinetic characterization of the ATPase cycle of the DnaK molecular chaperone. *Biochemistry* 37:596–607
- Santoro MG (2000) Heat shock factors and the control of the stress response. *Biochem Pharmacol* 59:55–63
- Schonfeld HJ, Behlke J (1998) Molecular chaperones and their interactions investigated by analytical ultracentrifugation and other methodologies. *Methods Enzymol* 290:269–296
- Swain JF, Dinler G, Sivendran R, Montgomery DL, Stotz M, Gierasch LM (2007) Hsp70 chaperone ligands control domain association via an allosteric mechanism mediated by the interdomain linker. *Mol Cell* 26:27–39
- Tavaria M, Gabriele T, Kola I, Anderson RL (1996) A hitchhiker's guide to the human Hsp70 family. *Cell Stress Chaperones* 1:23–28
- Teale FW (1960) The ultraviolet fluorescence of proteins in neutral solution. *Biochem J* 76:381–388
- Theyssen H, Schuster HP, Packschies L, Bukau B, Reinstein J (1996) The second step of ATP binding to DnaK induces peptide release. *J Mol Biol* 263:657–670
- Vogel M, Bukau B, Mayer MP (2006) Allosteric regulation of Hsp70 chaperones by a proline switch. *Mol Cell* 21:359–367
- Vogt G, Woell S, Argos P (1997) Protein thermal stability, hydrogen bonds, and ion pairs. *J Mol Biol* 269:631–643
- Wada K, Taniguchi A, Xu L, Okano T (2005) Rapid and highly sensitive detection of cadmium chloride induced cytotoxicity using the HSP70B' promoter in live cells. *Biotechnol Bioeng* 92:410–415
- Walmsley AR, Martin GE, Henderson PJ (1994) 8-Anilino-1-naphthalenesulfonate is a fluorescent probe of conformational changes in the D-galactose-H<sup>+</sup> symport protein of *Escherichia coli*. *J Biol Chem* 269:17009–17019
- Walter S, Buchner J (2002) Molecular chaperones—cellular machines for protein folding. *Angew Chem Int Ed Engl* 41:1098–1113
- Wang XY, Li Y, Yang G, Subjeck JR (2005) Current ideas about applications of heat shock proteins in vaccine design and immunotherapy. *Int J Hyperther* 21:717–722
- Wegele H, Muller L, Buchner J (2004) Hsp70 and Hsp90—a relay team for protein folding. *Rev Physiol Biochem Pharmacol* 151:1–44
- Wu B, Hunt C, Morimoto R (1985) Structure and expression of the human gene encoding major heat shock protein HSP70. *Mol Cell Biol* 5:330–341
- Wu SJ, Liu FH, Hu SM, Wang C (2001) Different combinations of the heat-shock cognate protein 70 (hsc70) C-terminal functional groups are utilized to interact with distinct tetratricopeptide repeat-containing proteins. *Biochem J* 359:419–426
- Zylicz M, King FW, Wawrzynow A (2001) Hsp70 interactions with the p53 tumour suppressor protein. *EMBO J* 20:4634–4638